Multigrid defect correction and fourth-order compact scheme for Poisson's equation

Stéphane Abide, Belkacem Zeghmati

Multigrid defect correction and fourth-order compact scheme for Poisson's equation

Stéphane Abide *, Belkacem Zeghmati

Laboratoire de Mathématiques et de Physique, Université de Perpignan Via Domitia, 52 Avenue Paul Alduy, 66860 Perpignan, France

This paper presents an analysis of a multigrid defect correction to solve a fourth-order compact scheme discretization of the Poisson's equation. We focus on the formulation, which arises in the velocity/pressure decoupling methods encountered in computational fluid dynamics. Especially, the Poisson's equation results of the divergence/gradient formulation and Neumann boundary conditions are prescribed. The convergence rate of a multigrid defect correction is investigated by means of an eigenvalues analysis of the iteration matrix. The stability and the mesh-independency are demonstrated. An improvement of the convergence rate is suggested by introducing the damped Jacobi and Incomplete Lower Upper smoothers. Based on an eigenvalues analysis, the optimal damping parameter is proposed for each smoother. Numerical experiments confirm the findings of this analysis for periodic domain and uniform meshes which are the working assumptions. Further numerical investigations allow us to extend the results of the eigenvalues analysis to Neumann boundary conditions and non-uniform meshes. The Hodge–Helmholtz decomposition of a vector field is carried out to illustrate the computational efficiency, especially by making comparisons with a second-order discretization of the Poisson's equation solved with a state of art of algebraic multigrid method.

1. Introduction

Since the early days of computing, many research works have been published on the development of numerical solutions of Poisson's equation. This elliptic partial differential equation has many applications in various areas of applied physics such as acoustic, electromagnetism, heat and mass transfer, etc. For instance, the Poisson solver is an essential part for solving incompressible fluid flows. In this case, the computational cost saving still remains of primary importance, that has led to an important amount of papers in this research area. The combination of a discrete spatial approximation and a linear solver is the key point of such methods of solutions for elliptic partial differential equations. For instance, the progress in multigrid methods has allowed us to achieve a good scalability for finite-element, finite-difference or finite-volume discretizations. In order to reduce the computational cost, yet another popular way is to discretize the equations with high-order schemes like the spectral methods. High-order methods achieve a better accuracy than lower-order discretizations with identical grid

* Corresponding author.
E-mail address: stephane.abide@univ-perp.fr (S. Abide).

size. The compact finite difference schemes belong to this category of high-order schemes. They have the particular feature to combine the accuracy with linear computational complexity. For this reason, the compact finite difference schemes have a good scaling potential. However, the combination of such discretizations with an efficient linear solver for elliptic boundary value problems still remains an open issue. In this way, the main objective of the present work is to propose an iterative method of solving the Poisson equation discretized based on a fourth-order compact finite difference schemes. A special care is paid to the singular Poisson equation arising from incompressible fluid flow solvers. Here the discrete formulation results from the combination of the discrete divergence with the discrete gradient. The Neumann boundary conditions are also considered.

The compact finite difference schemes achieve a high-order truncation error while keeping the smallest computational stencil. One of pioneer way to obtain those schemes consists in approximating the partial derivative equation with a second-order finite difference and in replacing the higher derivatives in the truncation error by the lower-order derivatives of equation itself. The well-known Mehrstellen discretization of the Poisson equation, proposed by Collatz [1], is among the first published papers relating to this procedure. A large amount of works follows this trend [2–10]. For instance, Spotz and co-workers proposed high-order compact schemes (HOCS) formulation for solving numerically the two-dimensional convection/diffusion equation [2], the three-dimensional Poisson equation [3], with extension to non-uniform grids [4]. The contributions to HOCS of Zhang and co-workers concern also elliptic boundary value problems [5–8]. A three-dimensional HOCS of the convection/diffusion equation was proposed [5]. Furthermore, an analytical mesh transformation was developed to deal with boundary layer type problems [6], and a transformation-free mesh of three-dimensional Poisson equation [7] was recently proposed. A six-order accuracy was achieved with the compact scheme presented by Wang and Zhang [8]. These works illustrated a first set of methods to design accurate multi-dimensional schemes for elliptic boundary value problems. The common feature is that they lead to a sparse linear system, which has to be solved efficiently. Iterative methods for the solution of linear systems of equations are usually used. The Krylov projection type methods [2] or multigrid methods [10,9] have been successfully developed. The recent geometric multigrid procedure designed by Wang and Zhang [8] has a convergence factor independent of the mesh size. This illustrates how compact finite difference schemes could combine accuracy with a linear computational complexity. In the framework of computational fluid dynamics, these schemes have been applied to the $\psi - \omega$ formulation of the incompressible Navier–Stokes equations [11,12]. It should be mentioned that in the computational fluid dynamics the Poisson's equation generally arises from the combination of gradient and divergence operators, especially with the class of projection methods [13,14].

Yet another popular way to derive the compact schemes is based on Taylor series expansions. Here linear combinations on the discrete derivative (interpolation) and the function involved are determined by fulfilling requirements on accuracy and/or resolution. The core of the method was detailed in the seminal paper of Lele [15], and still remains a starting point for many other high-order schemes [16–18]. Their derivations are based on a one-dimensional computational stencil. The multidimensional extension can be simply done by means of a tensor product. However, in this case, the resulting linear system of equations is not sparse which introduces several difficulties to get a solution efficiently, especially for Poisson equation arising in the incompressible fluid flow solvers [19,20]. Nevertheless, several direct and iterative methods of solutions have been used [21–24]. For instance, the diagonalization method, which was first used in combination with spectral methods [25], still remains retained as a method of solutions for linear systems arising from compact schemes discretization [22,26]. This direct method has an unfavorable computational complexity, and seems not to be suitable for large scale computing. An another way based on FFT leads to efficient numerical solvers, but it introduces some limitations on the number of stretching mesh directions [27,28]. The early work of Schiestel and Viazzo [23] introduces an iterative procedure between the momentum and the pressure correction equations. Their method is based on a variant of the defect correction method [29]. Knikker [24] suggested a defect correction procedure as method of solutions for the Poisson's equation discretized with a fourth-order compact finite difference scheme. The principle consists in solving a lower order accurate discretization of the Poisson's equation and in correcting the residual, which is computed using a higher-order discretization [29]. Introducing an under-relaxation coefficient, this iterative method has demonstrated the efficiency for the expected application, but no details concerning the convergence rate were specified. Such an analysis was given by Brüger et al. [30] for an iterative Krylov method preconditioned with an Incomplete Lower Upper (ILU) factorization. Since the matrix was not available explicitly, the ILU factorization concerned a second-order finite differences approximation of the Poisson equation. The analysis of the convergence factor showed a condition number which behaves as $o(h^{-1})$, h being the grid space.

The above review presents results of several works relating the efficiency of the Poisson solvers based on high-order compact schemes combined with multigrid. In these works, the Poisson equation did not arise from the combination of the discrete divergence and the gradient operators. For this reason, these methods are not applicable to the Poisson equation occurring in the incompressible fluid flow solvers. In this context, only few works considered such discretizations with an iterative linear solver, also there is a little amount of information on the convergence factor. In the present work, we are going to give some insights into defect correction applied to the Poisson equation with a particular focus on the convergence factor analysis. Yet another aim of this work is to show how the convergence factor can be improved by using a smoothing step. Section 1 deals with the spatial discretization and the analysis of the convergence factor of the defect correction method. Then several numerical experiments highlight the accuracy and the influence of the smoother operator on the convergence factor. The computational cost issues are also addressed with the Hodge–Helmholtz decomposition of a vector field, which mimics the pressure equation in incompressible fluid flow solvers.

2. Numerical methods

2.1. Fourth-order compact finite difference scheme

The two-dimensional Poisson equation with the Neumann boundary conditions is considered, viz.,

$$\begin{aligned} -\left(\partial_x\partial_x + \partial_y\partial_y\right)\phi &= f(x,y), \quad (x,y) \in \Omega, \\ \partial_{\mathbf{n}}\phi &= g(x,y), \quad (x,y) \in \partial\Omega, \end{aligned} \tag{1}$$

where Ω is a bounded domain and $\partial\Omega$ is the boundary of Ω. The solution ϕ, the forcing term f and the boundary values function g are assumed to be sufficiently smooth. This equation is defined on a square domain $\Omega = [0, 1] \times [0, 1]$ and a uniform mesh size $h_x = h_y = h = n^{-1}$ is considered. The function ϕ in Eq. (1) is defined on the nodes $(x_{i-1/2}, y_{j-1/2})$ with $x_{i-1/2} = (i - 1/2)h$ and $y_{j-1/2} = (j - 1/2)h$, where $1 \leq i, j \leq n$. This corresponds to the classical layout of pressure like variables on a staggered grid. According to the projection methods [13,14], the Poisson equation is built as the composition of the divergence and gradient operators. The operators are defined on the staggered grid. This implies that the gradient and the divergence are evaluated at the cell faces and at the cell centers, respectively. In particular, the components of the gradient operator are evaluated at the nodes $(x_i, y_{j-1/2})$ and $(x_{i-1/2}, y_j)$, whereas the discrete divergence is computed at the cell centers $(x_{i-1/2}, y_{j-1/2})$. The notation $\delta^{cf}_{x(y)}$ refers to the cartesian components of the gradient operator and $\delta^{fc}_{x(y)}$ refers to the derivatives involved in the divergence operator. Thus the discrete Poisson problem, expressed with tensorial notations, reads

$$-\left(\delta^{fc}_x\delta^{cf}_x \otimes I + I \otimes \delta^{fc}_y\delta^{cf}_y\right)\phi = f \tag{2}$$

with the following Neumann boundary conditions

$$\begin{cases} \delta^{cf}_x\phi\big|_{0,j-1/2} = g_{0,j-1/2} \\ \delta^{cf}_x\phi\big|_{n_x,j-1/2} = g_{n_x,j-1/2}, \end{cases} \qquad \begin{cases} \delta^{cf}_y\phi\big|_{i-1/2,0} = g_{i-1/2,0} \\ \delta^{cf}_y\phi\big|_{i-1/2,n_y} = g_{i-1/2,n_y}. \end{cases} \tag{3}$$

Each discrete derivative $\delta^{cf}_{x(y)}$ and $\delta^{fc}_{x(y)}$ is discretized with the fourth-order compact finite-difference. The *cell-to-face* derivative for the inner nodes is given by

$$\frac{1}{24}\phi'_{i-1} + \frac{11}{12}\phi'_i + \frac{1}{24}\phi'_{i+1} = \frac{1}{h}(\phi_{i+1/2} - \phi_{i-1/2}) + o\left(h^4\right), \tag{4}$$

and the *face-to-cell* corresponds to the shift version of Eq. (4)

$$\frac{1}{24}\phi'_{i-3/2} + \frac{11}{12}\phi'_{i-1/2} + \frac{1}{24}\phi'_{i+1/2} = \frac{1}{h}(\phi_i - \phi_{i-1}) + o\left(h^4\right). \tag{5}$$

The boundary nodes discretization of the *face-to-cell* derivative is

$$\phi'_{-1/2} + 23\phi'_{1/2} = \frac{1}{h}(26\phi_0 - 25\phi_1 + \phi_2) + o\left(h^3\right). \tag{6}$$

The *cell-to-face* derivative boundary relation is given by

$$\phi'_0 = \frac{1}{24h}(-23\phi_{-1/2} + 21\phi_{1/2} + 3\phi_{3/2} - \phi_{5/2}) + o\left(h^3\right). \tag{7}$$

Using Eqs. (4)–(7), each discrete derivative may be rewritten in the matrix form, viz.,

$$M^{cf}_{x(y)}\phi' = D^{cf}_{x(y)}\phi \quad \text{and} \quad M^{fc}_{x(y)}\phi' = D^{fc}_{x(y)}\phi. \tag{8}$$

With this notation, $M^{cf}_{x(y)}$ and $M^{fc}_{x(y)}$ are tridiagonal non singular matrices. The discrete fourth-order formulation of the Poisson equation is then

$$L'\phi = -\left[\left(M^{fc}_x\right)^{-1} D^{fc}_x \left(M^{cf}_x\right)^{-1} D^{cf}_x \otimes I + I \otimes \left(M^{fc}_y\right)^{-1} D^{fc}_y \left(M^{cf}_y\right)^{-1} D^{cf}_y\right]\phi = f. \tag{9}$$

The finite difference scheme for the boundary conditions Eq. (3) is

$$\begin{aligned} g_{0,j-1/2} &= \frac{1}{24h}(-23\phi_{-1/2,j-1/2} + 21\phi_{1/2,j-1/2} + 3\phi_{3/2,j-1/2} - \phi_{5/2,j-1/2}), \\ g_{n_x,j-1/2} &= -\frac{1}{24h}(-23\phi_{n_x+1/2,j-1/2} + 21\phi_{n_x-1/2,j-1/2} + 3\phi_{n_x-3/2,j-1/2} - \phi_{n_x-5/2,j-1/2}), \\ g_{i-1/2,0} &= \frac{1}{24h}(-23\phi_{i-1/2,-1/2} + 21\phi_{i-1/2,1/2} + 3\phi_{i-1/2,3/2} - \phi_{i-1/2,5/2}), \\ g_{i-1/2,n_y} &= -\frac{1}{24h}(-23\phi_{i-1/2,n_y+1/2} + 21\phi_{i-1/2,n_y-1/2} + 3\phi_{i-1/2,n_y-3/2} - \phi_{i-1/2,n_y-5/2}). \end{aligned} \tag{10}$$

Non-uniform meshes are considered via the introduction of an analytic mesh mapping. If $x(X)$ is a non singular mesh mapping, with X referring to the uniform mesh coordinates, a derivative is evaluated as $\delta_x = x_X^{-1}\delta_X$. For further details see Ref. [24]. It should be noted that the discrete operator L' is a dense matrix due to the inverses of $M^{cf}_{x(y)}$ and $M^{fc}_{x(y)}$. This makes difficult to develop efficient methods to solve Eq. (9), and specific strategies have to be drawn. The direct method of diagonalization may be used to solve Eqs. (9) and (10) [21], or by its multidomain extension [22]. Few iterative methods of solutions are available [30,24]. This way is investigated in the next section by considering an analysis of the multigrid defect correction method applied to Eqs. (9) and (10).

2.2. Convergence analysis of the defect correction

The multigrid defect correction solves the problem $L'\phi = c$ by means of an auxiliary problem $L\phi = c$ for which an efficient solution is available [29,31]. In our formulation, L' corresponds to the fourth-order discrete formulation described by Eqs. (9) and (10), which can be represented by a dense matrix, being evaluated with a linear time complexity. The auxiliary discrete problem L refers to the standard five-points stencil resulting in the second-order finite differences discretization of the Poisson equation Eq. (1). The defect correction method is based on the following iterative procedure

$$L\phi^{(k+1)} = L\phi^{(k)} - \left(L'\phi^{(k)} - f\right), \quad 1 \le k \le n. \tag{11}$$

The initial guess function $\phi^{(1)}$ is arbitrarily chosen. At a first sight, each defect iteration requires the solution of the auxiliary linear system L. However, as indicated in [31], one iteration of a multigrid solver is sufficient to ensure the convergence of the iterative procedure. This has been confirmed by our experience. The analysis of the convergence factor of this iterative process is based on the spectral radius of the iteration matrix $G_{std} = I - L^{-1}L'$. The convergence holds for a spectral radius of G strictly lower than 1, and the lowest spectral radius is suitable to obtain a better residual reduction rate, named convergence factor. The analytical calculation of the spectral radius becomes rapidly a cumbersome task. This is addressed by considering the following eigenfunctions [29]

$$\varphi(x, y) = e^{i\theta_x x/h} e^{i\theta_y y/h} \qquad -\pi \le \theta_x, \theta_y \le \pi. \tag{12}$$

If the periodic boundary conditions are assumed, the replacing (θ_x, θ_y) by $(k_x\pi h, k_y\pi h)$ is equivalent to consider a discrete spectrum, and the rigorous Fourier analysis theory is recovered. A direct computation of the eigenvalues of the five points second order and the fourth order discretization gives, accordingly,

$$L\varphi = \frac{4}{h^2}\left(1 - \frac{1}{2}\cos\theta_x - \frac{1}{2}\cos\theta_y\right)\varphi = \frac{4}{h^2} f_{2th}(\theta_x, \theta_y), \tag{13}$$

and

$$L'\varphi = \frac{4}{h^2}\left(\frac{\sin^2(\theta_x/2)}{\left(\frac{11}{12} + \frac{1}{12}\cos\theta_x\right)^2} + \frac{\sin^2\left(\theta_y/2\right)}{\left(\frac{11}{12} + \frac{1}{12}\cos\theta_y\right)^2}\right)\varphi = \frac{4}{h^2} f_{4th}(\theta_x, \theta_y). \tag{14}$$

The eigenvalues λ_{sf} of the iteration matrix $G_{sf} = I - L^{-1}L'$ are deduced from the relations

$$\lambda_{sf}(\theta_x, \theta_y) = 1 - f_{4th}(\theta_x, \theta_y)/f_{2th}(\theta_x, \theta_y). \tag{15}$$

Fig. 1 represents $|\lambda_{sf}|$ as a function of θ_x and θ_y.

This contour plot includes ten isovalues ranging from 0.05 to 0.40, which shows that the highest eigenvalues are located on the nodes $(\theta_x, \theta_y) = (0, \pm\pi)$ and $(\theta_x, \theta_y) = (\pm\pi, 0)$. So the following inequality is readily deduced:

$$|\lambda_{sf}| \le |\lambda(0, \pm\pi)| = |\lambda(\pm\pi, 0)| = \frac{11}{25}. \tag{16}$$

Since the eigenvalues are strictly lower than 1, the defected correction method is a convergent iterative procedure. Moreover, the convergence factor $q_{sf} = 11/25$ is independent of the grid parameter h. This feature is important to design an efficient method of solution because this is a prerequisite for the linear time algorithm. According to Fig. 1, the convergence factor is strongly governed by the high frequencies: the highest eigenvalues are located close to the domain's boundaries. A classical technique to improve the convergence factor consists in adding to the defect correction a smoothing sweep, which can be viewed as a preconditioner. In this case, the iterative procedure Eq. (11) becomes

$$\overline{\phi} = \phi^{(k)} - T\left(L'\phi^{(k)} - c\right), \tag{17}$$

$$L\phi^{(k+1)} = L\overline{\phi} - \left(L'\overline{\phi} - c\right). \tag{18}$$

The influence of the smoothing sweep T onto the convergence factor is examined for two cases: the damped Jacobi and ILU factorization. The relaxation operator modifies the iteration matrix as $G = (I - L^{-1}L')(I - TL)$. Its spectral radius governs

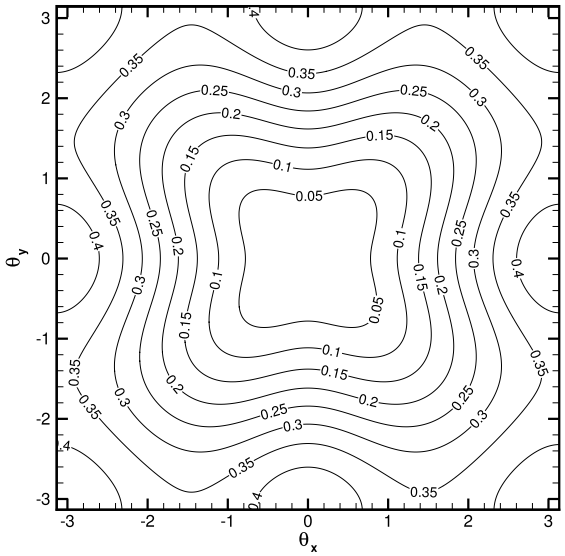

Fig. 1. Eigenvalues plot of the iteration matrix for the smoother-free defect correction.

the convergence factor of the whole procedure. Here, the Jacobi relaxation [29] is considered. It is based on the diagonal of the matrix L arising from the second-order discretization: $\omega h^2/4$. Indeed, the eigenvalues λ_{jac} are given by

$$\lambda_{jac}(\theta_x, \theta_y, \omega) = \lambda_{sf}(\theta_x, \theta_y)\left[1 - \omega f_{4th}(\theta_x, \theta_y)\right], \tag{19}$$

where ω is the relaxation factor. In a similar way, the formal eigenfunctions of the ILU smoothing operator are given by [32]

$$\frac{4}{h^2}\left(1 - \frac{1}{2}\cos\theta_x - \frac{1}{2}\cos\theta_y + \frac{1}{4+2\sqrt{2}}\cos(\theta_x + \theta_y)\right) = \frac{4}{h^2} f_{ilu}(\theta_x, \theta_y), \tag{20}$$

and, the eigenvalues of the iteration matrix are readily computed as

$$\lambda_{ilu}(\theta_x, \theta_y, \omega) = \lambda_{sf}(\theta_x, \theta_y)\left[1 - \omega\frac{f_{4th}(\theta_x, \theta_y)}{f_{ilu}(\theta_x, \theta_y)}\right]. \tag{21}$$

Conversely, the calculation of the spectral radius of the iteration matrix is defined as

$$\rho(\omega) = \max_{-\pi < \theta_x, \theta_y < \pi} \left|\lambda(\theta_x, \theta_y, \omega)\right|, \tag{22}$$

where the former notation holds for the damped Jacobi and ILU smoother. The spectral radius is a function of the relaxation factor ω, and might admit an optimal value which minimizes it. In this work, a numerical study is carried out to evaluate the optimal relaxation factor for the both smoothers. The convergence factor Eq. (22) is plotted in Fig. 2 for each smoother.

The figure clearly indicates the existence of a minimum which corresponds to the optimal relaxation factor. The spectral radius of the Jacobi smoother is minimal for $\omega_{jac} = 0.4763$, yielding a convergence factor $q_{jac} = 0.1635$ which is lower than the smoother-free method. The optimal relaxation factor of the ILU smoothing operator is $\omega_{ilu} = 0.6751$, and the associated convergence factor is $q_{ilu} = 0.0611$. To complete the description of the convergence properties, the contour plot of the eigenvalues for the optimal relaxation factor is represented in Fig. 3.

As the smoother-free method, these plots show that the highest eigenvalues are located in the high frequency range. It should be noted that the introduction of the smoothing operator improves the reduction factor of the defect correction. Thus, the ILU smoother gives a factor of improvement of 8 in comparison with the smoother-free method. We remind that a uniform periodic mesh is assumed in the former analysis, and that the knowledge of the behavior with the Neumann boundary conditions and non-uniform meshes is of major importance in practical applications. This aspect and the implementation verification are addressed in the next section by means of various numerical experiments.

Implementation details

The Neumann boundary conditions lead to a singular problem: the solutions of Poisson's equation are defined up to a constant. There are several methods to consider this special feature. In this work, it is addressed by imposing the Dirichlet condition on a unique boundary node in the auxiliary problem L. Next, both the discrete approximations L and L' are scaled by h^2, and the stopping criterion is the L^2-norm of the residual. The auxiliary problem L is not solved at each iteration of

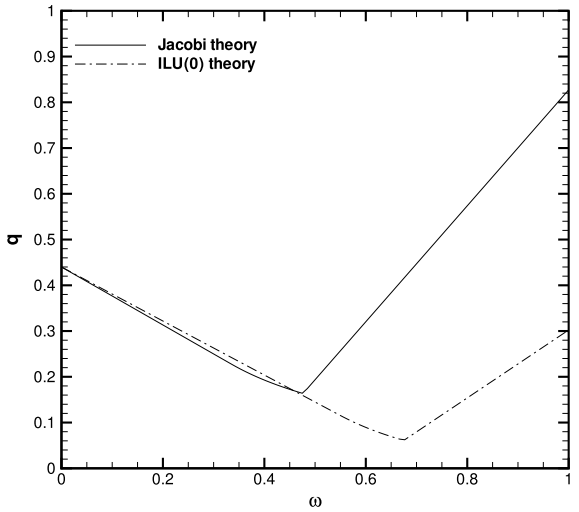

Fig. 2. Convergence factor q versus the relaxation factor ω.

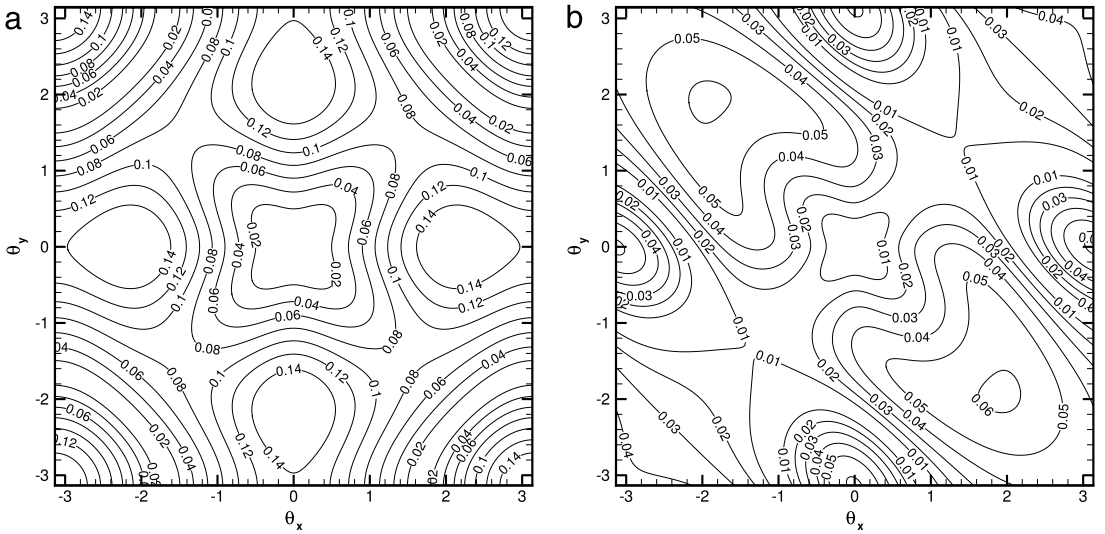

Fig. 3. Eigenvalues plot of the iteration matrix for the Jacobi (a) and the ILU (b) smoothers.

the defect correction. More particularly, only one iteration of a multigrid method is sufficient to get the convergence of the defect correction. Here, the Algebraic Multigrid method (AMG) provided by the HYPRE library is used. The ILU decomposition smoother, is also provided by the HYPRE library. The fill-in level set to zero (ILU(0)) corresponds to the above mentioned analysis. In the numerical experiments, the fill-in level dependency on the convergence factor is investigated, in this case associated notation is ILU(k).

3. Numerical experiments

In this section, several numerical experiments are carried out to validate the proposed multigrid defect correction. The fourth-order accuracy of the Poisson solver is first demonstrated. Then, the influence of the smoothing operator and the relaxation parameter on the convergence factor are outlined. In the last section, the Hodge–Helmholtz decomposition is considered to illustrate how the proposed defected correction is able to deal efficiently with the Poisson equation arising from simulations of incompressible fluid flow.

3.1. Spatial accuracy

The multigrid defect correction introduces a second-order finite difference discretization for the auxiliary problem, whereas the defect is evaluated via a higher accurate scheme. When the defect is converged, the high-order accurate

Table 1
Numerical *L2*-error and order of accuracy with a uniform mesh.

N	Problem 1		Problem 2		Problem 3		Problem 4	
	ϵ	p	ϵ	p	ϵ	p	ϵ	p
128	2.63e−09	0.00	2.42e−08	0.00	4.77e−09	0.00	1.40e−07	0.00
256	1.60e−10	4.04	2.04e−09	3.57	3.89e−10	3.62	2.48e−08	2.50
512	9.85e−12	4.02	1.74e−10	3.55	3.25e−11	3.58	4.40e−09	2.50
1024	6.12e−13	4.01	1.50e−11	3.54	2.75e−12	3.56	7.78e−10	2.50
2048	2.12e−14	4.85	1.29e−12	3.53	2.16e−13	3.67	1.38e−10	2.50

Table 2
Numerical *L2*-error and order of accuracy with a non-uniform mesh.

N	Problem 1		Problem 2		Problem 3		Problem 4	
	ϵ	p	ϵ	p	ϵ	p	ϵ	p
128	6.51e−06	0.00	1.49e−05	0.00	1.28e−06	0.00	6.32e−07	0.00
256	3.99e−07	4.03	8.74e−07	4.09	3.95e−08	5.02	1.47e−07	2.10
512	2.44e−08	4.03	5.20e−08	4.07	1.93e−09	4.35	3.82e−08	1.95
1024	1.51e−09	4.02	3.14e−09	4.05	1.30e−10	3.89	8.68e−09	2.14
2048	9.33e−11	4.01	1.92e−10	4.04	8.73e−12	3.90	1.91e−09	2.18

approximation is expected. This important feature is assessed by computing the order of accuracy p from the numerical errors computed with several mesh sizes. The following set of four problems is considered [27]:

1. $\phi\,(x, y) = (xy)^{3.5}\,[1 - \cos\,(xy)]$ (five times differentiable),
2. $\phi\,(x, y) = x^{4.5} + y^{4.5}$ (four times differentiable),
3. $\phi\,(x, y) = (x + y)^{2.5} \sin\,(x)$ (three times differentiable),
4. $\phi\,(x, y) = (x + y)^{2.5}$ (two times differentiable).

The order of differentiability of these solutions is between 2 and 5. The computations are performed on a unit square domain, and both uniform and non-uniform meshes are considered. The non-uniform mesh is obtained from the following analytical mapping

$$x(X) = X + \beta \sin\,[(8X + 1)\pi\,]\,, \tag{23}$$

where X stands for the uniform mesh of size $h = n^{-1} = n_x^{-1} = n_y^{-1}$ and where the parameter β is determined to prescribe the smallest space step $h_{\min} = 0.6h$. The metrics $x_X = x'(X)$ and $y_Y = y'(Y)$ are determined from the analytical mesh transform Eq. (23). The order of accuracy is computed from the *L2*-error denoted ϵ_n which is the root mean square of the numerical error on a grid of size n. The order of accuracy p is computed as $p = \log_{10}\left(\epsilon_{n_1}/\epsilon_{n_2}\right) / \log_{10}\,(n_1/n_2)$ for the problems (1)–(4). Section 2 details three variants of the multigrid defect correction: the Jacobi and ILU smoothers and the smoother-free one. Preliminary computations show that the three methods give identical solutions with the machine accuracy precision. Thus, for the sake of clarity, only the numerical errors computed with the smoother-free version are presented.

Tables 1 and 2 present the numerical error as a function of the mesh size for each problem. Table 1 refers to the error computed on the uniform mesh. The numerical error shows that the order of accuracy achieves the expected fourth-order only with the solution (1).

As noted by Zhuang and Sun [27], the order decreases accordingly to the order of differentiability of the solution in the other cases. Table 2 lists the numerical errors on the non-uniform meshes.

As for the previous test with uniform mesh, the use of non-uniform meshes and sufficiently fine meshes leads to a similar conclusion: the scheme is fourth-order accurate except for the problem 4. These findings demonstrate that the present defect multigrid method retains the fourth-order accuracy on both uniform and non-uniform meshes. The next section investigates the convergence factor of the three different versions of the defect correction method.

3.2. Convergence factor of the multigrid defect correction

Section 2 details the multigrid defect correction and the benefit on the convergence factor in introducing a smoother. The theoretical convergence factor was derived from a uniform mesh and a periodic domain assumptions. The existence of an optimal relaxation factor ω for the Jacobi and the ILU smoothers has been demonstrated. In this section, several numerical experiments are first carried out to validate the theoretical predictions, and then to assess their validity out of the range of validity inherent in postulated assumptions. Thus, the above discussion is based on the convergence properties which include the convergence factor q, and the defect reductions d^k at iterations k. The defect reduction is computed as suggested by Trottenberg et al. [31]. The solution $u = 0$ of the homogeneous Poisson's problem $f = 0$ is considered, and the initial

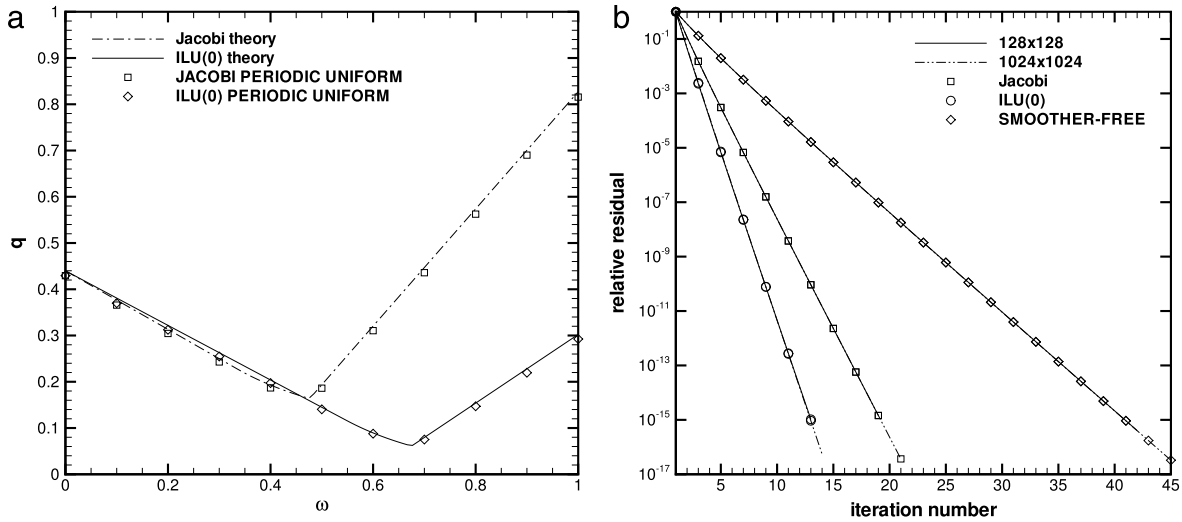

Fig. 4. Convergence factor versus relaxation factor (a), defect reduction versus the iteration number (b) with periodic boundary conditions and uniform meshes.

guess of the multigrid defect correction is initialized with a random field of zero mean value. The empirical convergence factor is computed from the defects at the iterations $m_0 = 10$ and $m_1 = 20$, with the relation

$$q = \sqrt[m_1 - m_0]{d^{m_1}/d^{m_0}}. \tag{24}$$

The optimal relaxation factor is computed from the minimum of the curve representing the convergence factor q as a function of the relaxation factor ω. Once, the optimal relaxation factor is determined for the Jacobi and the ILU(0) smoothers, their associated defect d^k versus the iteration numbers are considered for the two grid sizes 128×128 and 1024×1024. The defect of the smoother-free version $\omega = 0$ is also considered on these two grids. This allows us to evaluate the mesh-independency of the present method. From the relaxation factor and the defect data, we are able to assess the convergence features of the present multigrid defect correction.

Fig. 4 presents the convergence features, on a periodic domain with uniform mesh, of the multigrid defect correction for smoother-free, Jacobi and ILU(0) smoothers. It should be noted from Fig. 4(a) that the convergence factor q with respect to the relaxation parameter ω is in good agreement with the predictions of Section 2. The computed convergence factors are close to the analytical curves (full and dashed line) in the whole range of the relaxation factor. This allows us to validate the value of the optimal relaxation factor and tour numerical implementation. Next, Fig. 4(b) outlines the mesh-independency of the defect reduction for the three versions. Indeed, the defects reduction rate is identical regardless of the mesh size. It can be stated that the ILU(0) has the best defect reduction factor, as demonstrated in the former section.

Fig. 5 presents the convergence features when the periodic boundary conditions are substituted by Neumann ones. So, the assumptions made for the analytical derivation of the convergence factor are not valid. However, Fig. 5(a) shows that the computed convergence factors fit with theoretical ones for the Jacobi and the ILU(0) smoothers. Fig. 5(b) also shows the mesh-independency of the three implemented versions. From these remarks, the Neumann boundary conditions seem to be effect-less on the convergence features.

Fig. 6 presents the convergence properties for a periodic domain with a non-uniform mesh. In this case this is the mesh which does not fulfill the initial assumptions. This times, the convergence factor at the optimal relaxation factor is altered for both the Jacobi and the ILU(0) smoothers. In fact, the convergence factor is, respectively, about 0.3 and 0.15 for the Jacobi and ILU(0) smoothers in contrast to 0.18 and 0.08 as previously observed. Only the smoother-free version ($\omega = 0$) conserves a convergence close to 0.44. The defect convergence history for the Jacobi and ILU(0) smoothers are also affected: to reach the stopping criteria, few iterations are needed. This feature involves a slight loss of the mesh-independency.

In the same way, Fig. 7 shows the influence on the convergence factor of the Neumann boundary conditions associated with a non-uniform mesh. In this case all the initial assumptions are avoid. The curves follow the same trend observed in the periodic/non-uniform configuration. The convergence factor at the optimal relaxation factor is degraded and a loss of the mesh-independency of the defect reduction is noted. Thus it can be concluded that for the singular Poisson problem the convergence factor is strongly influenced by a non-uniform mesh.

Here, the influence of the fill-in parameter for the ILU smoother is investigated.

The convergence properties as a function of the fill-in parameter are detailed in Fig. 8 when Neumann boundary conditions and non-uniform mesh are considered. An important improvement is noted when the fill-in parameter increases. In Fig. 8(a), ILU(2), ILU(4) and ILU(10) give a better convergence factor than the ILU(0). Moreover, the optimal relaxation factor $\omega_{opt}^{ilu} = 0.6751$ predicted by theory is recovered by using ILU(2). In comparison with ILU(2), ILU(4) and ILU(10) do not lead to a more efficient scheme within the meaning of convergence factor.

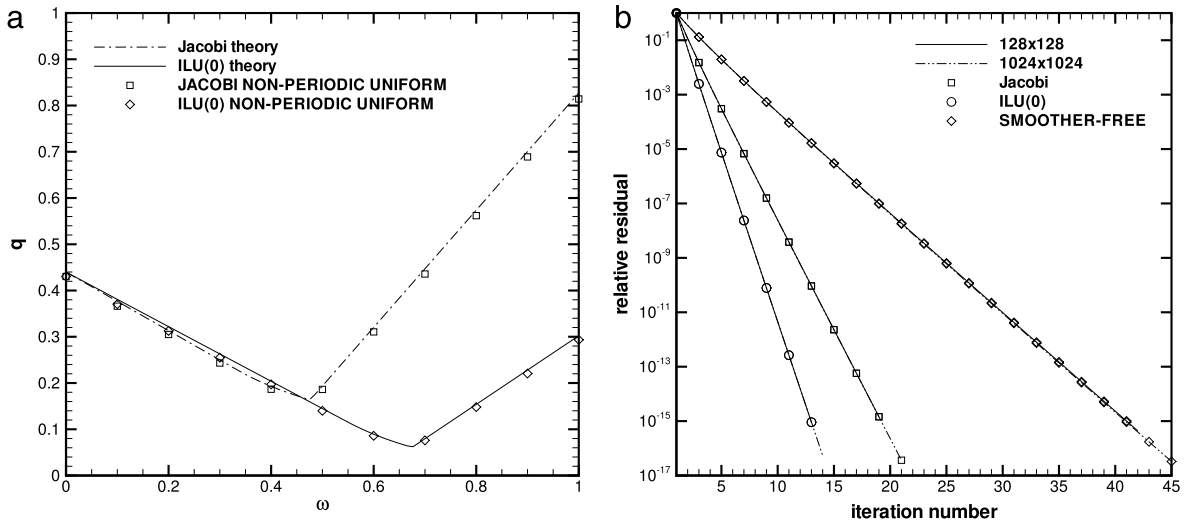

Fig. 5. Convergence factor versus relaxation factor (a), defect reduction versus the iteration number (b) with Neumann boundary conditions and uniform meshes.

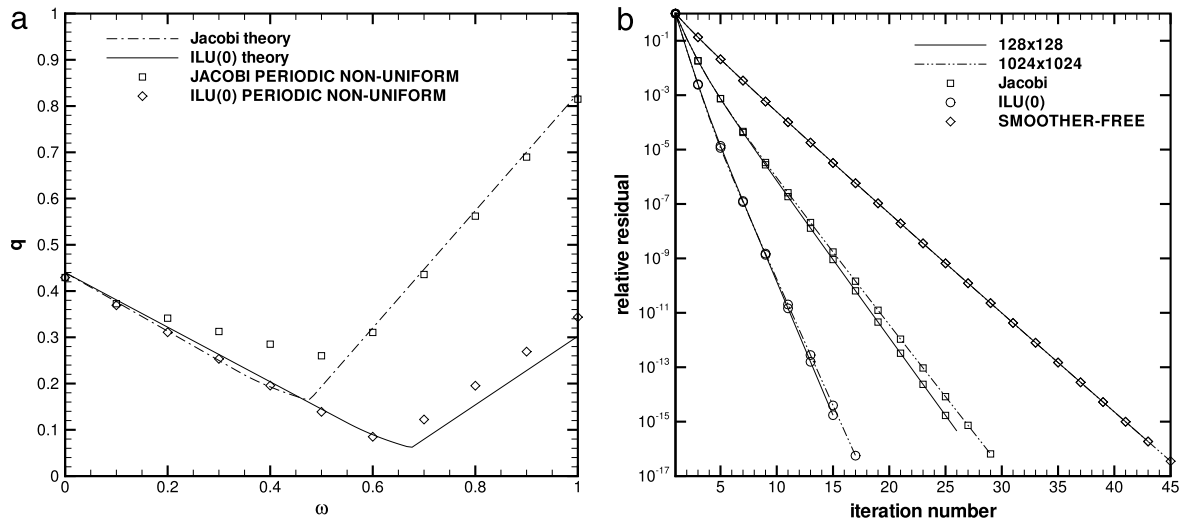

Fig. 6. Convergence factor versus relaxation factor (a), defect reduction versus the iteration number (b) with periodic boundary conditions and non-uniform meshes.

Regardless of the computational cost issue, the following conclusions can be drawn. First, the numerical experiments show that predicted optimal relaxation factors are in agreement with those computed, at least with non-uniform meshes. If non-uniform meshes are considered the optimal relaxation factors are altered, but can be recovered if ILU(4) is considered for the smoothing step. From the theory and the numerical experiments, there follows a clear conclusion: the defect correction associated with the ILU(4) smoother is the best combination in the meaning of the convergence factor. The complementary side of the computational cost issue is addressed in the next section. The computational time of the present multigrid defect correction is analyzed within a framework closed to the computational fluid dynamics: the Hodge–Helmholtz decomposition.

3.3. Hodge–Helmholtz decomposition of a vector field

A vector field can be decomposed as the sum of a divergence free vector field and a conservative vector field as follows

$$\mathbf{u}^{\star} = \mathbf{u} + \nabla\phi, \tag{25}$$

where $\nabla \cdot \mathbf{u} = 0$ and ϕ stands for a scalar field. In computational fluid dynamics of the incompressible flows, a such decomposition is a key point to obtain an approximate velocity fulfilling divergence-free constraint with the machine

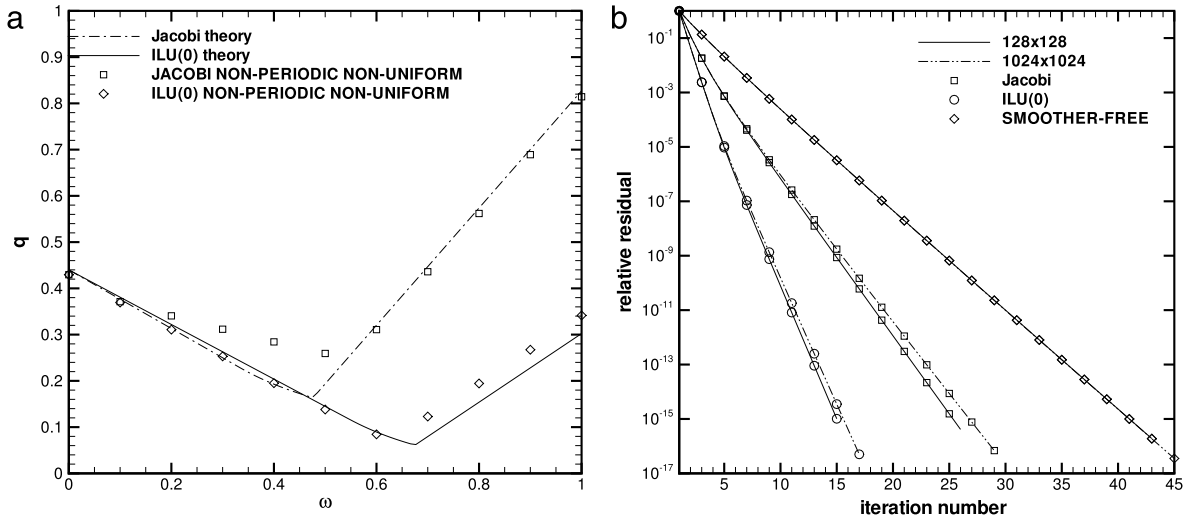

Fig. 7. Convergence factor versus relaxation factor (a), defect reduction versus the iteration number (b) with periodic boundary conditions and non-uniform mesh.

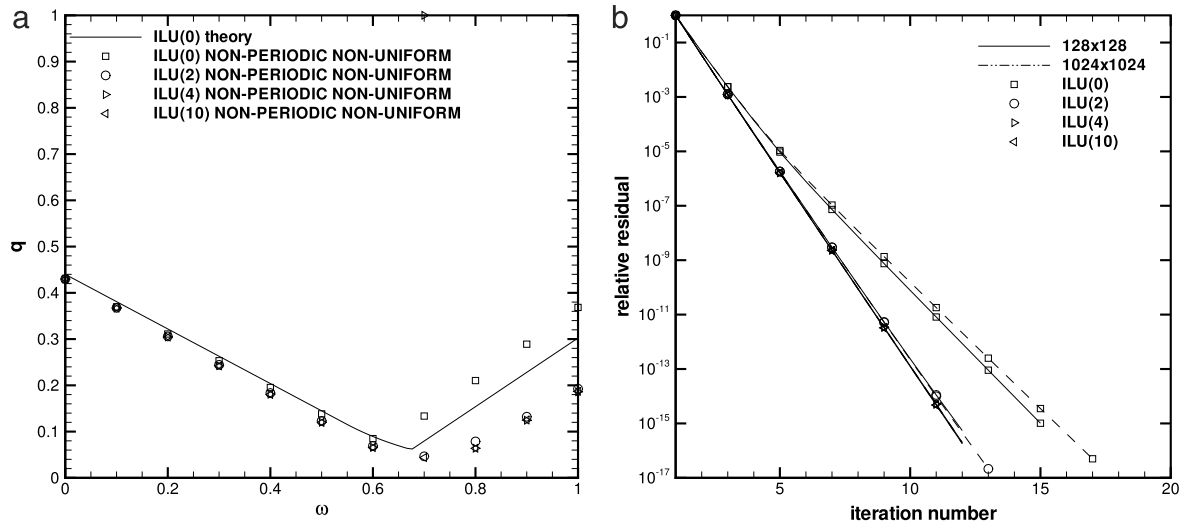

Fig. 8. Influence of the fill-in parameter; convergence factor versus relaxation factor (a), defect reduction versus the iteration number (b).

accuracy. Taking the divergence of the decomposition Eq. (25), the following Poisson equation is formulated

$$\nabla \cdot \nabla \phi = \nabla \cdot \mathbf{u}^{\star}. \tag{26}$$

Here, homogeneous Neumann boundary conditions are considered. The computational efficiency of the multigrid defect correction is evaluated with the decomposition of the following vector velocity field

$$\mathbf{u}^{\star} = (-\cos(2\pi x)\sin(2\pi y) + \pi \sin(4\pi x), \sin(2\pi x)\cos(2\pi y) + \pi \sin(4\pi y)) . \tag{27}$$

The Hodge–Helmholtz decomposition is given by

$$\begin{cases} \phi = -\dfrac{1}{4}\left(\cos(4\pi x) + \cos(4\pi y)\right) \\ \mathbf{u} = (-\cos(2\pi x)\sin(2\pi y), \sin(2\pi x)\cos(2\pi y)) . \end{cases} \tag{28}$$

The Neumann boundary conditions and the non-uniform mesh Eq. (23) are also considered. The stopping criterion is set to 10^{-10}. In order to investigate the performance of the multigrid defect correction, the absolute numerical error ϵ of the pressure ϕ, is plotted as a function of the CPU-time in Fig. 9(a).

This figure provides two major informations: the order of accuracy of the scheme and the dependency of the computational time with the grid size. For instance, if a scheme of order p ($\epsilon \propto h^p$) has a linear complexity algorithm

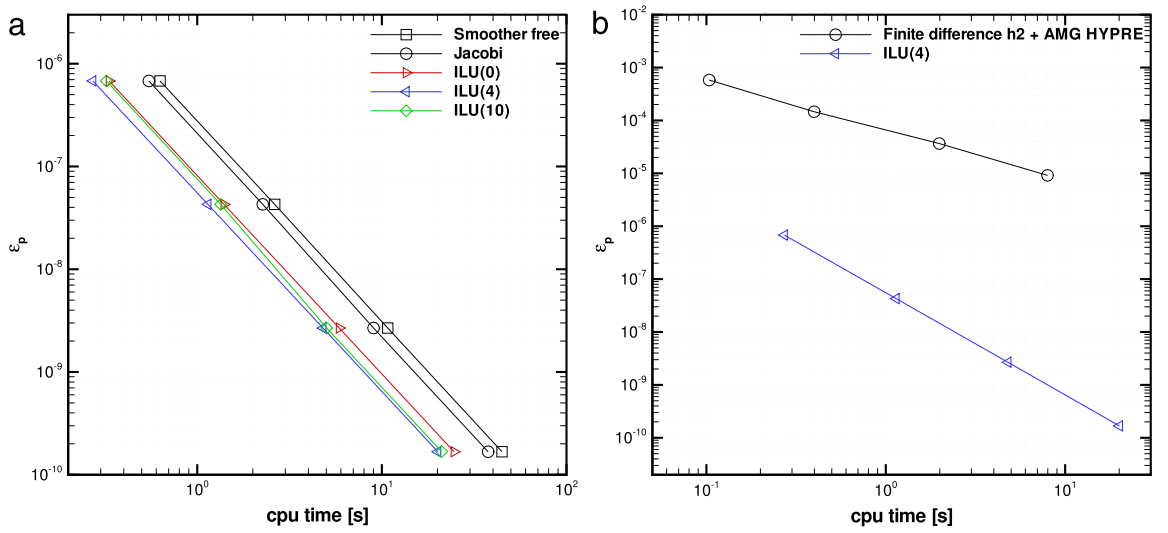

Fig. 9. Numerical error on ϕ versus cpu time, for different smoother (a), comparison with the second-order discretization (b).

($t_{cpu} \propto n^2 \propto 1/h^2$), then the numerical error varies with the computational time according to $\epsilon \propto t_{cpu}^{-p/2}$. Fig. 9(a) illustrates this feature for the smoother-free, Jacobi, ILU(4) and ILU(10) smoothers. First, independently on the smoother, slopes range in 1.8–1.9. This confirms the fourth-order accuracy of the scheme and the linear complexity algorithm of this method of solutions. This figure also illustrates that the most efficient smoother is the ILU(4) one. For instance, an error of the order of 10^{-7} is reached with the ILU(4) smoother with more than twice less computational resource than the smoother-free version. It should be also noted that the ILU(10) smoother needs a slightly more computational resource than the ILU(4) one for similar results for the largest mesh. This is in agreement with the conclusion of the previous section. Finally, comparisons between the ILU(4) smoother and a second order discretization of Poisson equation solved by the algebraic multigrid solver of HYPRE are provided in Fig. 9(b). The numerical error as a function of the computational time is plotted. First, the slope associated with the second order is about -1 as expected. Then, for this test case, the plot clearly shows the superiority of the fourth-order defect correction with the ILU(4) smoother associated with a multigrid Poisson solver. Indeed, the error level of the fourth-order is never achieved by the second-order discretization, at least with a reasonable cpu time.

4. Conclusion

In this work, a multigrid defect correction method is investigated to solve a fourth-order compact scheme approximation of the singular Poisson equation. An eigenvalues analysis of the iteration matrix is developed, and provides several insights on the convergence factor and the mesh-independency of the spectral radius. It is demonstrated that the introduction of a smoothing sweep improves the convergence factor of the iterative method, the latter being dependent on a relaxation factor. A procedure is proposed to determine the optimal value of this relaxation factor both for the Jacobi and ILU smoothers. The better convergence factor has been found for the ILU smoother: a factor of improvement of 8 is determined with the ILU smoother in comparison with the smoother-free version. This analysis is based on the assumption of a periodic domain and uniform mesh. Several numerical experiments were performed. First, the fourth-order accuracy is demonstrated on the uniform and non-uniform meshes with the Neumann boundary conditions. Then, the experiments on the uniform meshes corroborate the existence of an optimal relaxation factor for each smoother and the mesh-independency of the convergence factor. It has been found that a non-uniform mesh alterates the optimal convergence factor and the mesh-independency if the Jacobi and the ILU(0) smoothers are used. Furthermore, the smoother ILU(4) allows us to recover the theoretical convergence factor and the mesh independency. Finally, the computational performance is assessed by means of the Hodge–Helmholtz decomposition test case. It clearly shows that within the meaning of computational effort, the fourth-order accurate scheme is better than second order, thanks to the proposed efficient multigrid defect correction.

References

[1] L. Collatz, The Numerical Treatment of Differential Equations, in: Grundlehren der Mathematischen Wissenschaften, Springer-Verlag, 1960.
[2] W.F. Spotz, High-Order compact finite difference schemes for computational mechanics (Ph.D. thesis), University of Texas at Austin, 1995.
[3] W.F. Spotz, G.F. Carey, A high-order compact formulation for the 3D Poisson equation, Numer. Methods Partial Differential Equations 12 (2) (1996) 235–243.
[4] W.F. Spotz, Formulation and experiments with high-order compact schemes for nonuniform grids, Internat. J. Numer. Methods Heat Fluid Flow 8 (3) (1998) 288–303.
[5] M.M. Gupta, J. Zhang, High accuracy multigrid solution of the 3D convection diffusion equation, Appl. Math. Comput. 113 (2000) 249–274.

[6] L. Ge, J. Zhang, High accuracy iterative solution of convection diffusion equation with boundary layers on nonuniform grids, J. Comput. Phys. 171 (2) (2001) 560–578.
[7] Y. Ge, F. Cao, J. Zhang, A transformation-free HOC scheme and multigrid method for solving the 3D Poisson equation on nonuniform grids, J. Comput. Phys. 234 (234) (2013) 199–216.
[8] Y. Wang, J. Zhang, Sixth order compact scheme combined with multigrid method and extrapolation technique for 2D Poisson equation, J. Comput. Phys. 228 (1) (2009) 137–146.
[9] M.M. Gupta, J. Kouatchou, J. Zhang, Comparison of second- and fourth-Order discretizations for multigrid Poisson solvers, J. Comput. Phys. 132 (2) (1997) 226–232.
[10] A.L. Pardhanani, W.F. Spotz, G.F. Carey, A stable multigrid strategy for convection–diffusion using high order compact discretization, Electron. Trans. Numer. Anal. 6 (1997) 211–223.
[11] J. Zhang, Numerical simulation of 2D square driven cavity using fourth-order compact finite difference schemes, Comput. Math. Appl. 45 (1–3) (2003) 43–52.
[12] W.F. Spotz, G.F. Carey, High-Order compact scheme for the steady stream-function vorticity equations, Int. J. Numer. 38 (1995) (1995) 3497–3515.
[13] R. Temam, Une méthode d'approximation des solutions des équations Navier Stokes, Bull. Soc. Math. France 96 (1968) 115–152.
[14] A.J. Chorin, Numerical solution of the Navier Stokes equations, Math. Comp. 22 (104) (1968) 745–762.
[15] S.K. Lele, Compact finite difference schemes with spectral-like resolution, J. Comput. Phys. 103 (1) (1992) 16–42.
[16] H. Fu, Z. Wang, Y. Yan, C. Liu, Modified weighted compact scheme with global weights for shock capturing, Comput. & Fluids 96 (96) (2014) 165–176.
[17] P.C. Chu, C. Fan, A three-point sixth-order staggered combined compact difference scheme, Math. Comput. Modelling 32 (3–4) (2000) 323–340.
[18] Q. Zhou, Z. Yao, F. He, M. Shen, A new family of high-order compact upwind difference schemes with good spectral resolution, J. Comput. Phys. 227 (2) (2007) 1306–1339.
[19] J. Guermond, P. Minev, J. Shen, An overview of projection methods for incompressible flows, Comput. Methods Appl. Mech. Engrg. (ISSN: 0045-7825) 195 (44–47) (2006) 6011–6045.
[20] C. Pozrikidis, A note on the regularization of the discrete PoissonNeumann problem, J. Comput. Phys. 172 (2) (2001) 917–923.
[21] E. Vedy, S. Viazzo, R. Schiestel, A high-order finite difference method for incompressible fluid turbulence simulations, Internat. J. Numer. Methods Fluids 42 (11) (2003) 1155–1188.
[22] S. Abide, S. Viazzo, A 2D compact fourth-order projection decomposition method, J. Comput. Phys. 206 (1) (2005) 252–276.
[23] R. Schiestel, S. Viazzo, A Hermitian-Fourier Numerical method for solving the incompressible Navier–Stokes equations, Comput. & Fluids 24 (6) (1995) 739–752.
[24] R. Knikker, Study of a staggered fourth-order compact scheme for unsteady incompressible viscous flows, Internat. J. Numer. Methods Fluids 59 (10) (2009) 1063–1092.
[25] C. Canuto, M.Y. Hussaini, A.M. Quarteroni, A. Thomas Jr., et al., Spectral Methods in Fluid Dynamics, Springer Science & Business Media, 2012.
[26] A. Tyliszczak, A high-order compact difference algorithm for half-staggered grids for laminar and turbulent incompressible flows, J. Comput. Phys. 276 (2014) 438–467.
[27] Y. Zhuang, X.-H. Sun, A high-order fast direct solver for singular Poisson equations, J. Comput. Phys. 171 (1) (2001) 79–94.
[28] S. Laizet, E. Lamballais, J. Vassilicos, A numerical strategy to combine high-order schemes, complex geometry and parallel computing for high resolution {DNS} of fractal generated turbulence, Comput. & Fluids 39 (3) (2010) 471–484.
[29] Defect Corrections and Multigrid Iterations, in: Lecture Notes in Mathematics, vol. 960, Springer, 1981.
[30] A. Brüger, B. Gustafsson, P. Lötstedt, J. Nilsson, High order accurate solution of the incompressible NavierStokes equations, J. Comput. Phys. 203 (1) (2005) 49–71.
[31] U. Trottenberg, C. Oosterlee, A. Schüller, Multigrid, Academic Press, ISBN: 9780127010700, 2001.
[32] P. Wesseling, An Introduction to Multigrid Methods, in: Pure and Applied Mathematics, Wiley, 1992.